

Supplementary Materials for MicroRNAs Differentially Regulated by Akt Isoforms Control EMT and Stem Cell Renewal in Cancer Cells

Dimitrios Iliopoulos, Christos Polytarchou, Maria Hatziapostolou, Filippos Kottakis,
Ioanna G. Maroulakou, Kevin Struhl, Philip N. Tsichlis*

*To whom correspondence should be addressed. E-mail: ptsichlis@tuftsmedicalcenter.org

Published 13 October 2009, *Sci. Signal.* **2**, ra62 (2009)
DOI: 10.1126/scisignal.2000356

This PDF file includes:

- Fig. S1. Abundance of the three Akt isoforms in spontaneously immortalized lung fibroblasts transduced with retroviral constructs of Akt1, Akt2, or Akt3 and in primary lung fibroblasts from wild type mice.
- Fig. S2. Heat map of differentially expressed microRNAs in untreated and IGF-1-treated fibroblasts, expressing no Akt (TKO), or individual Akt isoforms.
- Fig. S3. Validation of microRNA microarray data by SYBR Green real-time RT-PCR analysis in Akt1-, Akt2-, and Akt3-expressing fibroblasts.
- Fig. S4. Abundance of miR-200a and miR-200c in spontaneously immortalized lung fibroblasts from *Akt1^{fl/fl}/Akt2^{-/-}/Akt3^{-/-}* mice transduced with MigR1-GFP constructs of Akt1, Akt2, or Akt3 and MigR1-RFP-Cre.
- Fig. S5. Down-regulation of miR-200 microRNA family members in myrAkt2-expressing cells.
- Fig. S6. Akt1, Akt2 and Akt3 phosphorylation by IGF-1 is not affected by overexpression of miR-200a, miR-200c, or miR-200a plus miR-200c.
- Fig. S7. TGF β treatment (20 ng/ml) induces Akt phosphorylation (at Ser⁴⁷³) in MCF10A mammary epithelial cells and in murine lung fibroblasts expressing each of the three Akt isoforms.
- Fig. S8. MCF10A cells have similar amounts of Akt1 and Akt2.
- Fig. S9. Akt1 and Akt2 have opposing effects on the induction of EMT.
- Fig. S10. The knockdown of Akt1 enhances cell motility, whereas the knockdown of Akt2 does not.
- Fig. S11. Genomic localization of miR-200 family members. miR-200b, miR-200a and miR-429 map in a cluster on chromosome 1, and miR-200c and miR-141, map in a second cluster on chromosome 12.
- Fig. S12. The knockdown of Akt1 decreases the abundance of all the members of the miR-200 microRNA family.

Fig. S13. The abundance of miR-200a, and the mRNAs encoding Zeb1, and Zeb2 in MCF10A cells transfected with Akt1 siRNA, returned to the pretransfection values as the effects of the Akt1 siRNA on Akt1 abundance wane.

Fig. S14. Expression of Akt1 and Akt2 in adherent and non-adherent MCF10A cells treated with siRNAs for Akt1 and/or Akt2 (harvested on the 6th day of culture at passage 5).

Fig. S15. E-cadherin and vimentin mRNA abundance in MCF10A cells, harvested at consecutive days of culture in suspension.

Fig. S16. MMTV-cErbB2-induced mammary adenocarcinomas express miR-200c and E-cadherin.

Fig. S17. MMTV-cErbB2/*Akt1*^{-/-} mammary adenocarcinomas have more Zeb1 and vimentin and less E-cadherin than mammary adenocarcinomas developing in MMTV-cErbB2/*Akt1*^{+/+} and MMTV-cErbB2/*Akt2*^{-/-} mice.

Table S1. The microRNA signatures of immortalized lung fibroblasts expressing a single Akt isoform at a time and responding to IGF-1 differ.

Table S2. Comparison of the microRNA signatures of triple Akt knockout (TKO) lung fibroblasts, and their derivatives expressing Akt1, Akt2 or Akt3.

References

Supporting Online Material

**MicroRNAs differentially regulated by Akt isoforms control EMT
and stem cell renewal in cancer cells**

Dimitrios Iliopoulos ^{1*}, Christos Polytarchou ^{2*}, Maria Hatzia Apostolou ²,
Filippos Kottakis ², Ioanna G. Maroulakou ², Kevin Struhl ¹, Philip N. Tsichlis ^{2,3}

¹ Department of Biological Chemistry and Molecular Pharmacology, Harvard
Medical School, Boston, MA.

² Molecular Oncology Research Institute, Tufts Medical Center, Boston, MA

Contents

Supporting Figures.....	2
Supporting Tables.....	20
Supporting References.....	24

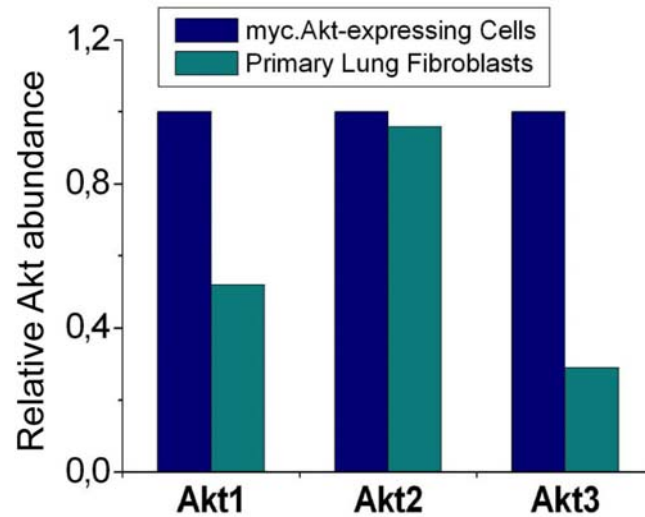


Fig. S1. Abundance of the three Akt isoforms in spontaneously immortalized lung fibroblasts transduced with retroviral constructs of Akt1, Akt2, or Akt3 and in primary lung fibroblasts from wild type mice. Western blots of cell lysates were probed with the indicated Akt1-, Akt2-, or Akt3-specific antibodies. Tubulin was used as loading control. Protein bands were measured by densitometry.

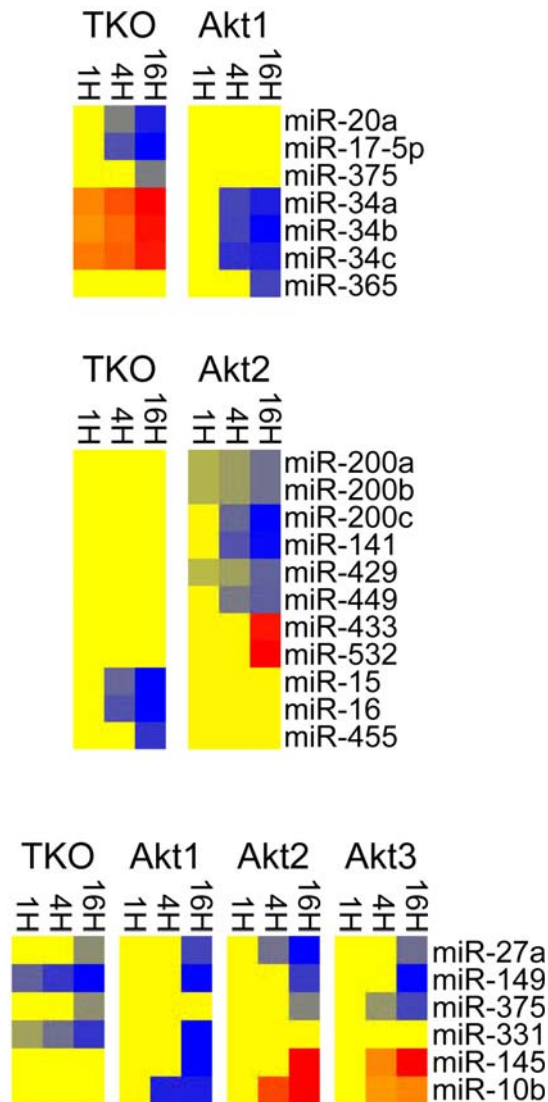


Fig. S2. Heatmap of differentially expressed microRNAs in untreated and IGF1-treated fibroblasts, expressing no Akt (TKO), or individual Akt isoforms. Red color indicates up-regulation, and blue color indicates down-regulation. The three panels show microRNAs that are upregulated or downregulated differentially in response to IGF1, in TKO and Akt1-expressing cells (upper panel), TKO and Akt2-expressing cells (middle panel), and TKO and Akt1-, Akt2-, and Akt3-expressing cells (lower panel) (see also table S2).

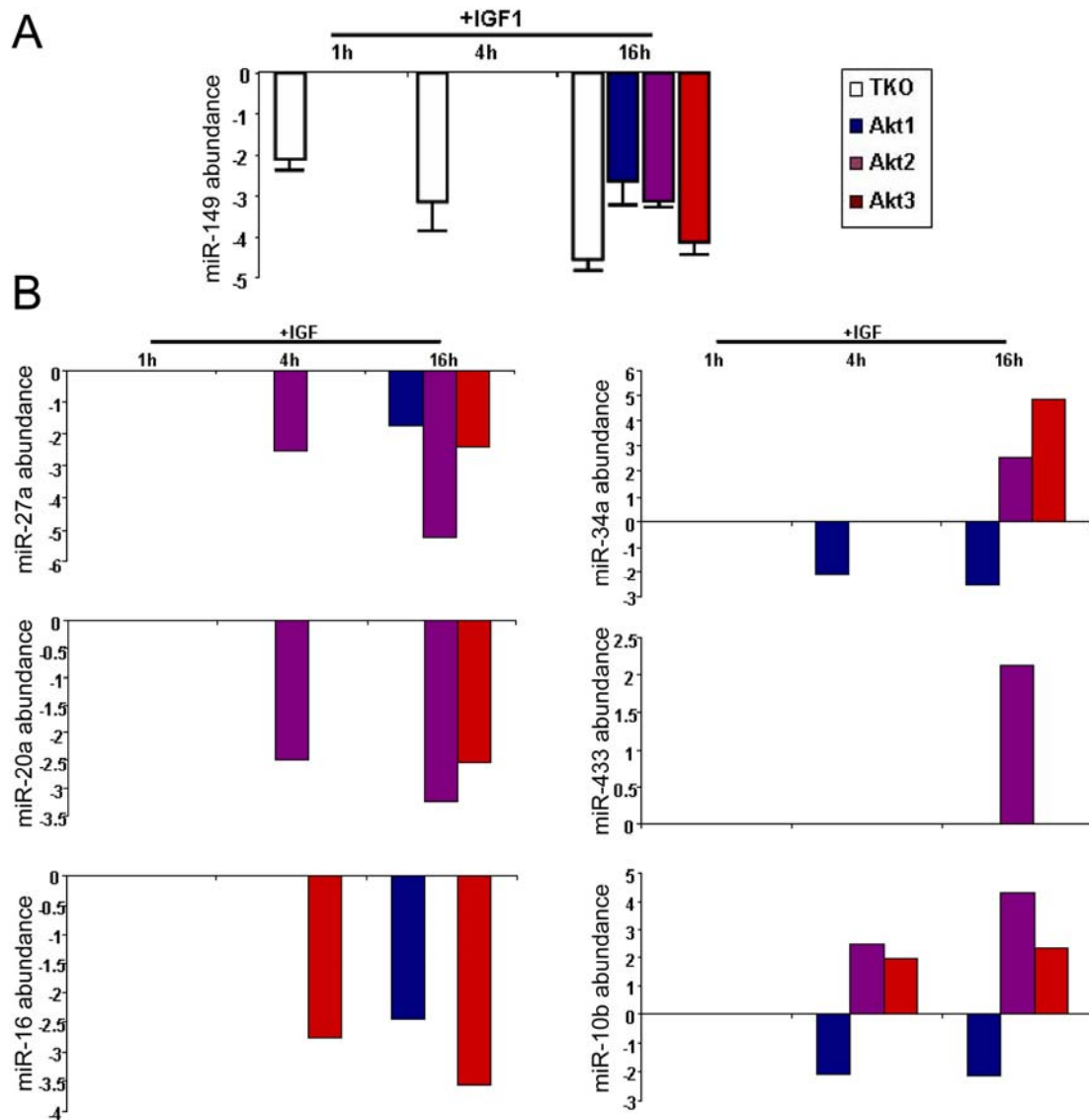


Fig. S3. Validation of microRNA microarray data by SYBR Green Real-time RT-PCR analysis in Akt1-, Akt2-, and Akt3-expressing fibroblasts. After overnight serum starvation cells were treated with IGF1 (50 ng/ml) and harvested 1, 4, or 16h later. This figure shows IGF1-induced changes in abundance of representative examples of Akt-regulated microRNAs. **(A)** Quantitative differences in the downregulation of miR-149 by IGF1, in TKO and Akt1, Akt2, or Akt3-expressing immortalized lung fibroblasts. **(B).** Quantitative and qualitative

differences in the regulation of miR-27a, miR-20a, miR-16, miR-34a, miR-433 and miR-10b by IGF1, in immortalized lung fibroblasts engineered to express Akt1, Akt2 and Akt3.

The data in A and B validate the microRNA microarray data and confirm the dynamics of microRNA expression during IGF1 treatment in cells expressing different Akt isoforms.

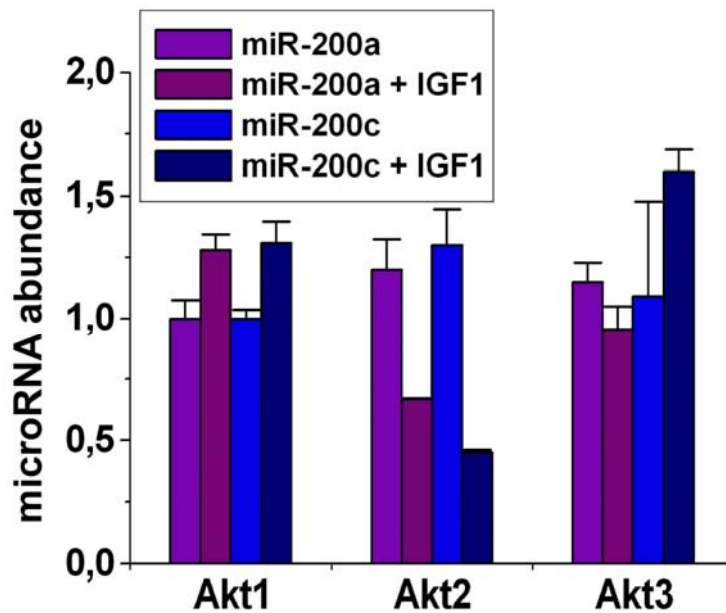


Fig. S4. Abundance of miR-200a and miR-200c in spontaneously immortalized lung fibroblasts from *Akt1^{fl/fl}/Akt2^{-/-}/Akt3^{-/-}* mice transduced with MigR1-GFP constructs of Akt1, Akt2, or Akt3 and MigR1-RFP-Cre. The abundance of miR-200a and miR-200c was measured 16 hours following IGF1 treatment (50 ng/ml), by real time RT-PCR. MiR-200 family members were downregulated upon IGF1 treatment only in Akt2-expressing fibroblasts. The experiment was performed in triplicate and data are presented as mean \pm SD.

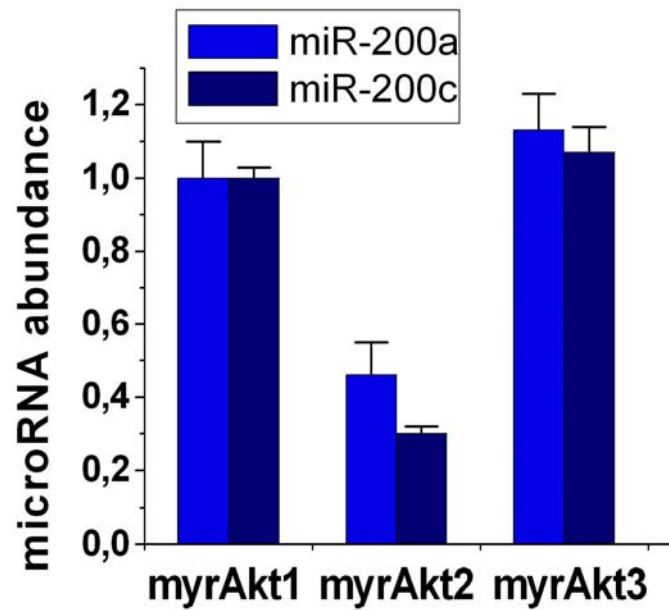


Fig. S5. Downregulation of miR-200 microRNA family members in myrAkt2-expressing cells. The abundance of miR-200a and miR-200c was measured by real time RT-PCR in serum-starved cells transduced with pBabe-puro-based constructs of myrAkt1, myrAkt2 or myrAkt3. Data are presented as mean \pm SD.

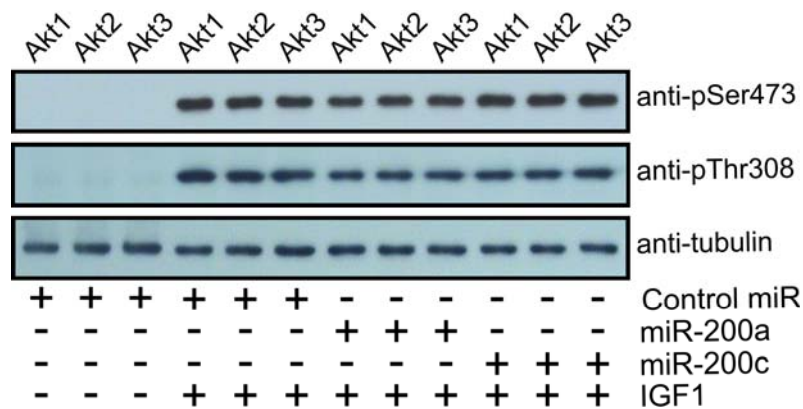


Fig. S6. Akt1, Akt2 and Akt3 phosphorylation by IGF1 is not affected by overexpression of miR-200a, miR-200c, or miR-200a plus miR-200c. Akt1, Akt2 and Akt3 expressing fibroblasts were transfected with control miR, miR-200a or miR-200c. After overnight serum-starvation, transfected cells were stimulated with IGF1 (50 ng/ml) for 10 min. Western blots of cell lysates were probed with the indicated phosphospecific antibodies. Tubulin was used as loading control.

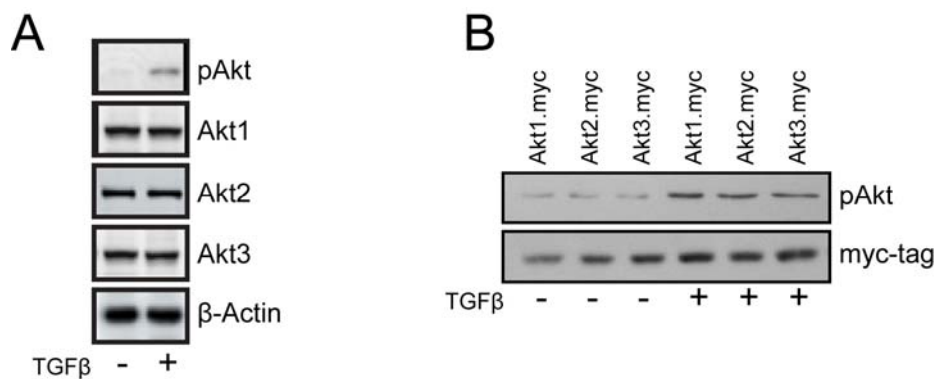


Fig. S7. TGF β treatment (20 ng/ml) induces Akt phosphorylation (at Ser473) (**A**) in MCF10A mammary epithelial cells and (**B**) in murine lung fibroblasts expressing each of the three Akt isoforms.

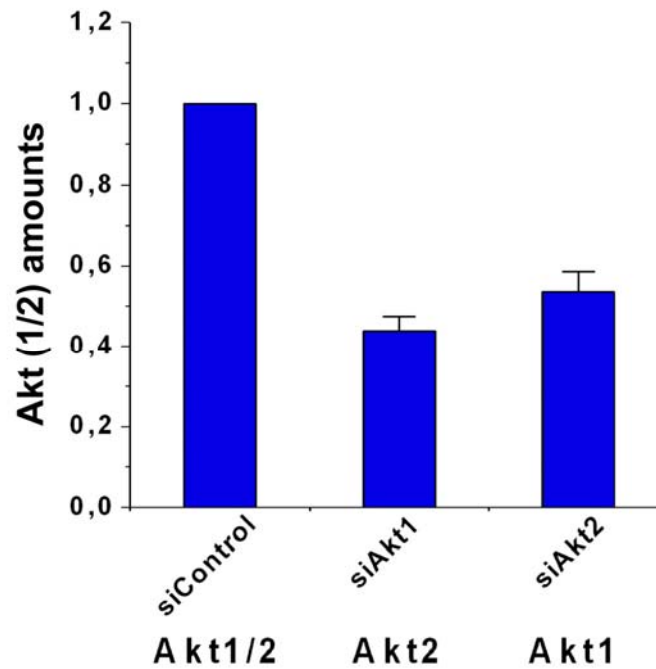


Fig. S8. MCF10A cells have similar amounts of Akt1 and Akt2. Cells were transfected with control siRNA or siRNAs for Akt1 and Akt2 (50 nM) and were analyzed by real time RT-PCR for the expression of Akt1 and Akt2 using primers that detect both Akt1 and Akt2 but not Akt3. The Akt detected in cells transfected with siControl represents the total amount of Akt1 plus Akt2. This was set to a value of 1. The Akt detected in siAkt1 and siAkt2-transfected cells represents the total Akt2 or Akt1 respectively. Their values added together equal approximately 1. Data are presented as mean \pm SD.

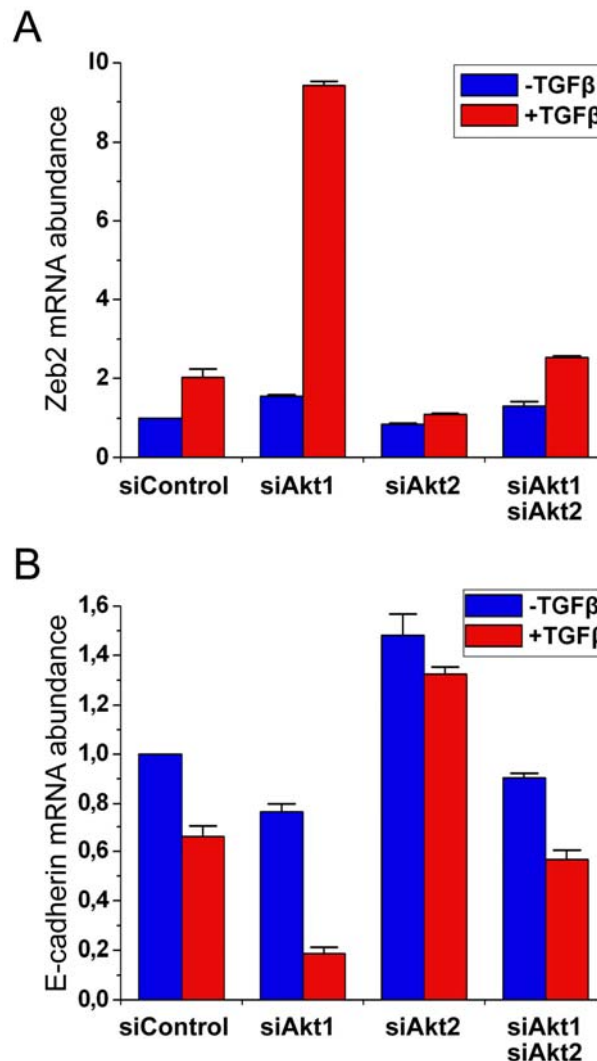


Fig. S9. Akt1 and Akt2 have opposing effects on the induction of EMT. **(A)** Zeb2, similar to Zeb1 (Fig 2B), is increased in response to Akt1 knockdown and TGF β treatment. Knockdown of Akt2 -not only does not induce Zeb2- but also abolishes the effects of the Akt1 knockdown. Real-time RT-PCR analysis showing the abundance of mRNA encoding Zeb2 in untreated and TGF β -treated (20 ng/ml) MCF10A cells transfected with a control siRNA, or siRNAs targeting Akt1, Akt2, or Akt1 plus Akt2 (50 nM). The induction of Zeb2 was more robust in cells in which Akt1 was knocked down. **(B)** Whereas the knockdown of Akt1 decreases

the abundance of the mRNA encoding E-cadherin, the knockdown of Akt2 does not. Moreover, the knockdown of Akt2 abolishes the effects of the Akt1 knockdown. Expression of E-cadherin in untreated and TGF β -treated MCF10A cells transfected with control, Akt1, Akt2, or Akt1 plus Akt2 siRNAs, was examined by real-time RT-PCR. The experiments were performed in triplicate and data are presented as mean \pm SD.

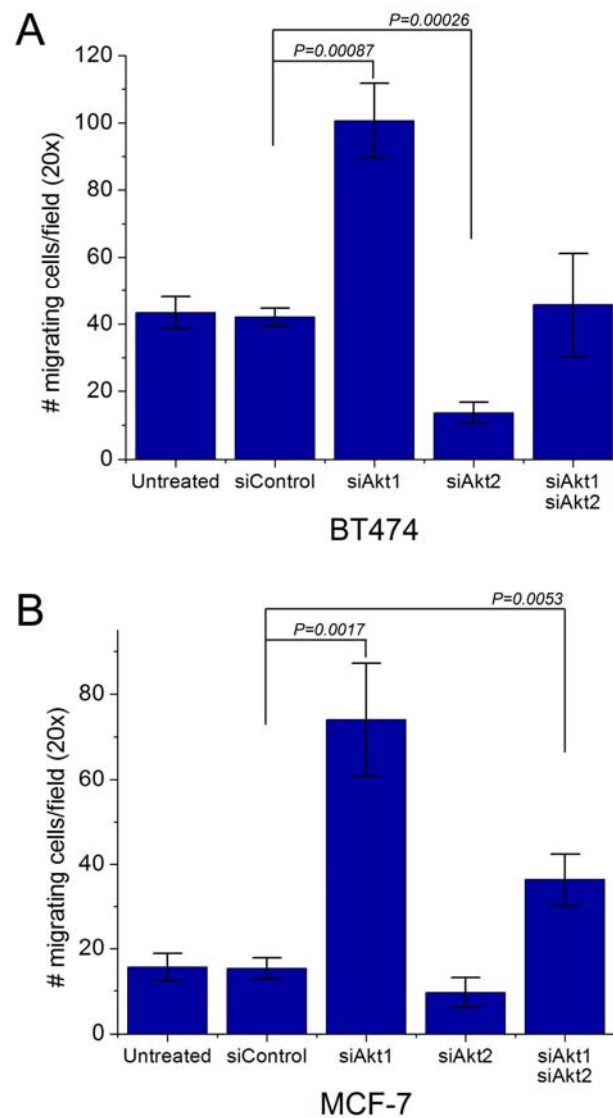


Fig. S10. The knockdown of Akt1 enhances cell motility, whereas the knockdown of Akt2 does not. Furthermore, the knockdown of Akt2 abolishes the effects of Akt1 knockdown on cell motility. Cell motility was measured via transwell migration assays on **(A)** BT474 and **(B)** MCF-7 cells 24h after transfection with control, Akt1, Akt2, or Akt1 plus Akt2 siRNAs. The experiments were performed in triplicate and data are presented as mean \pm SD.

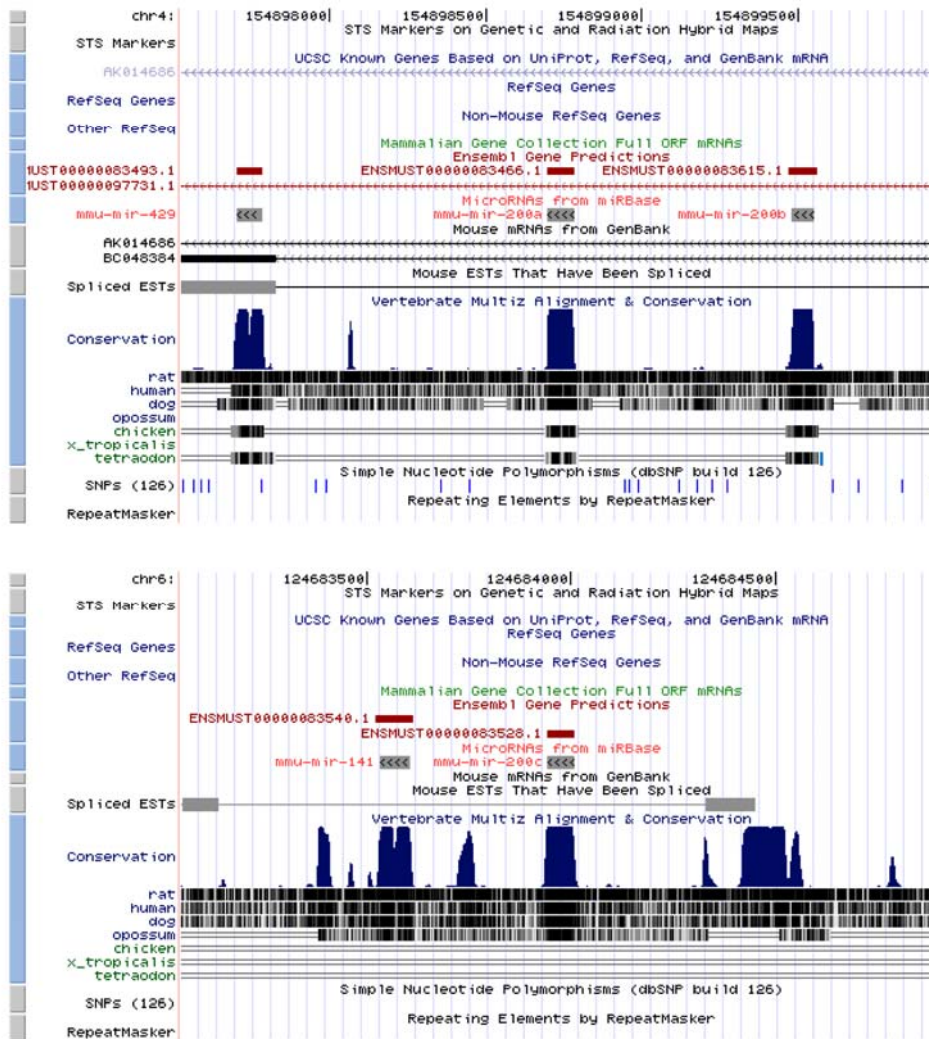


Fig. S11. Genomic localization of miR-200 family members. miR-200b, miR-200a and miR-429 map in a cluster on chromosome 1, and miR-200c and miR-141, map in a second cluster on chromosome 12. The genomic localization of the miR-200 microRNA family members was determined, using the UCSC Genome Browser (version Mar. 2006). Comparative analysis of the miR-200 family in vertebrates suggests high conservation of the clustering and of their seed sequences.

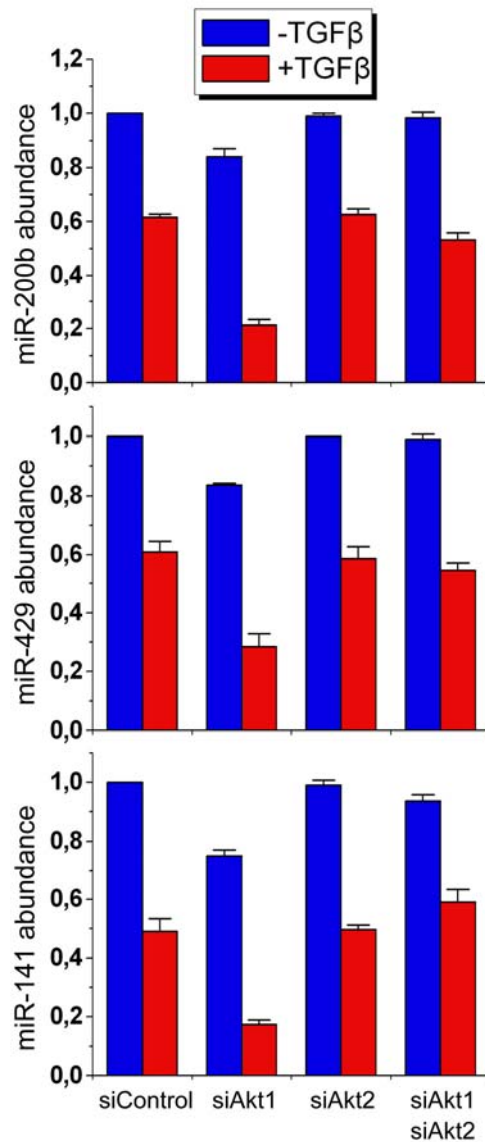


Fig. S12. The knockdown of Akt1 decreases the abundance of all the members of the miR-200 microRNA family. Real time RT-PCR shows that the knockdown of Akt1 promotes the decrease of all the members of the miR-200 microRNA family in MCF10A cells treated with TGFβ (20 ng/ml for 24 hours). Knockdown of Akt2 -not only does not downregulate the miR-200 microRNAs- but also abolishes the effects of Akt1 knockdown. The experiments were performed in triplicate and data are presented as mean \pm SD.

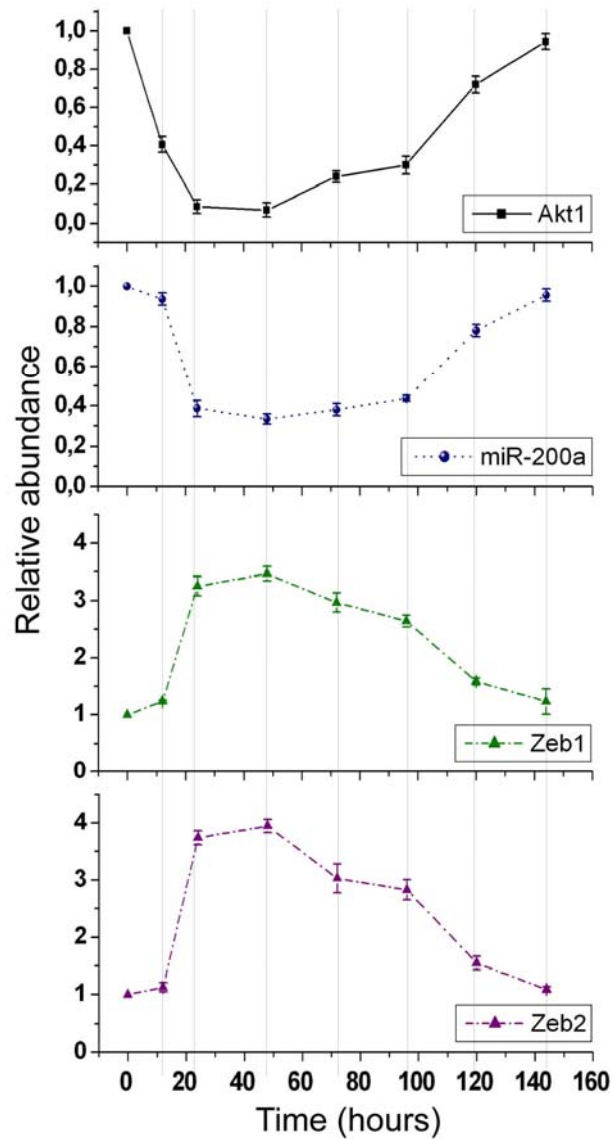


Fig. S13. The abundance of miR-200a, and the mRNAs encoding Zeb1, and Zeb2 in MCF10A cells transfected with Akt1 siRNA, returned to the pretransfection values as the effects of the Akt1 siRNA on Akt1 abundance wane. Time course analysis by real-time RT-PCR of the levels of miR-200a, Zeb1 and Zeb2 in MCF10A cells transfected with Akt1 siRNA and treated with TGF β .

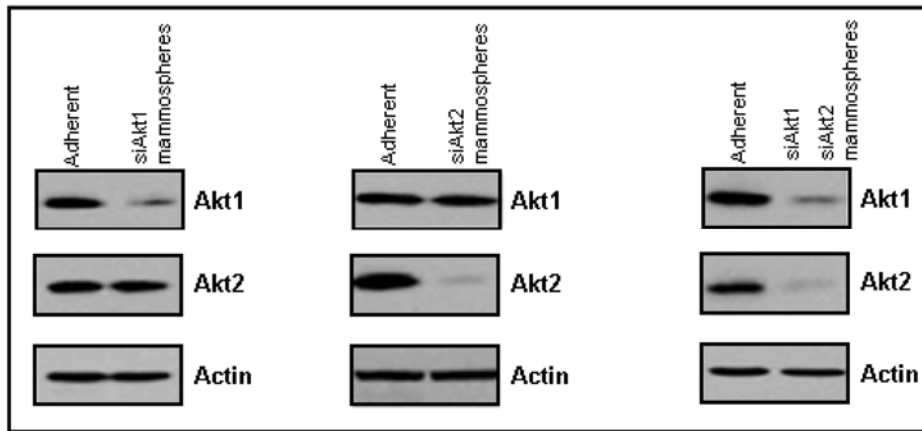


Fig. S14. Expression of Akt1 and Akt2 in adherent and non-adherent MCF10A cells treated with siRNAs for Akt1 and/or Akt2 (harvested on the 6th day of culture at passage 5). Mammosphere cells continue to show low amounts of Akt1 and/or Akt2, six days after transfection of the corresponding siRNAs. Beta actin levels were used as the loading control.

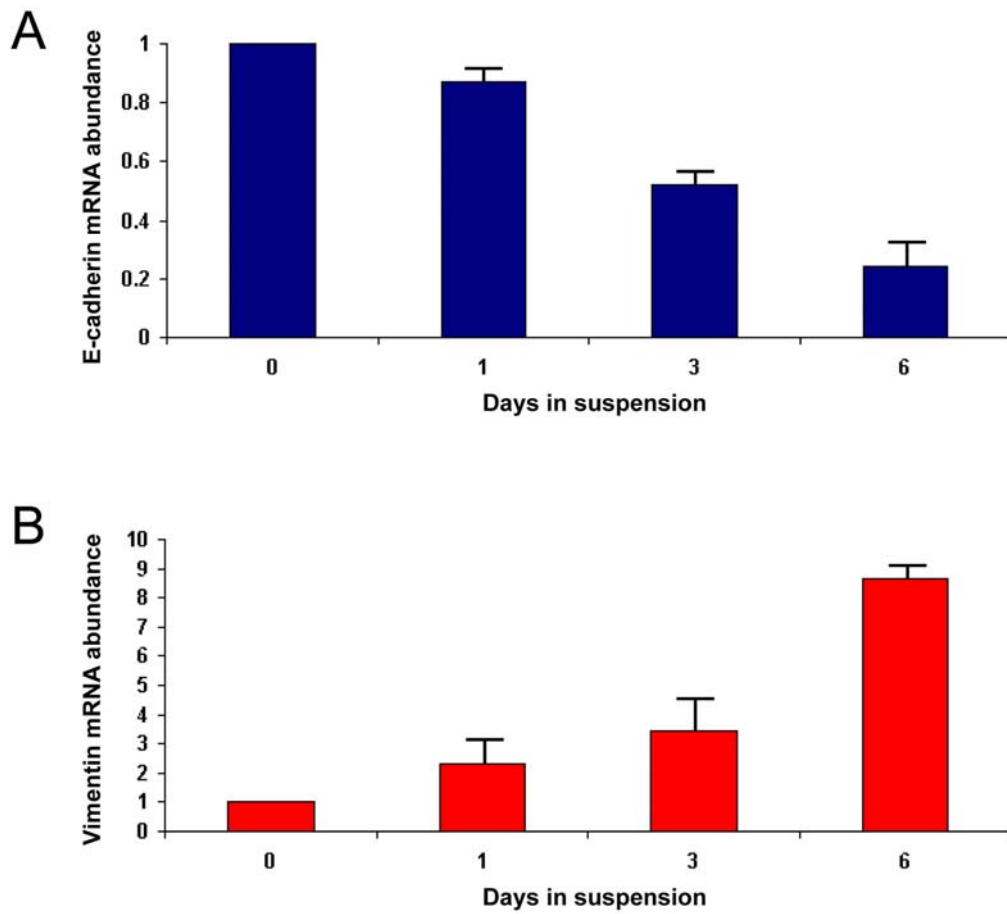


Fig. S15. E-cadherin and Vimentin mRNA abundance in MCF10A cells, harvested at consecutive days of culture in suspension. Cells were transfected with Akt1 siRNA and were cultured in media containing TGF β (20ng/ml). Cells at day 0 are adherent cells.

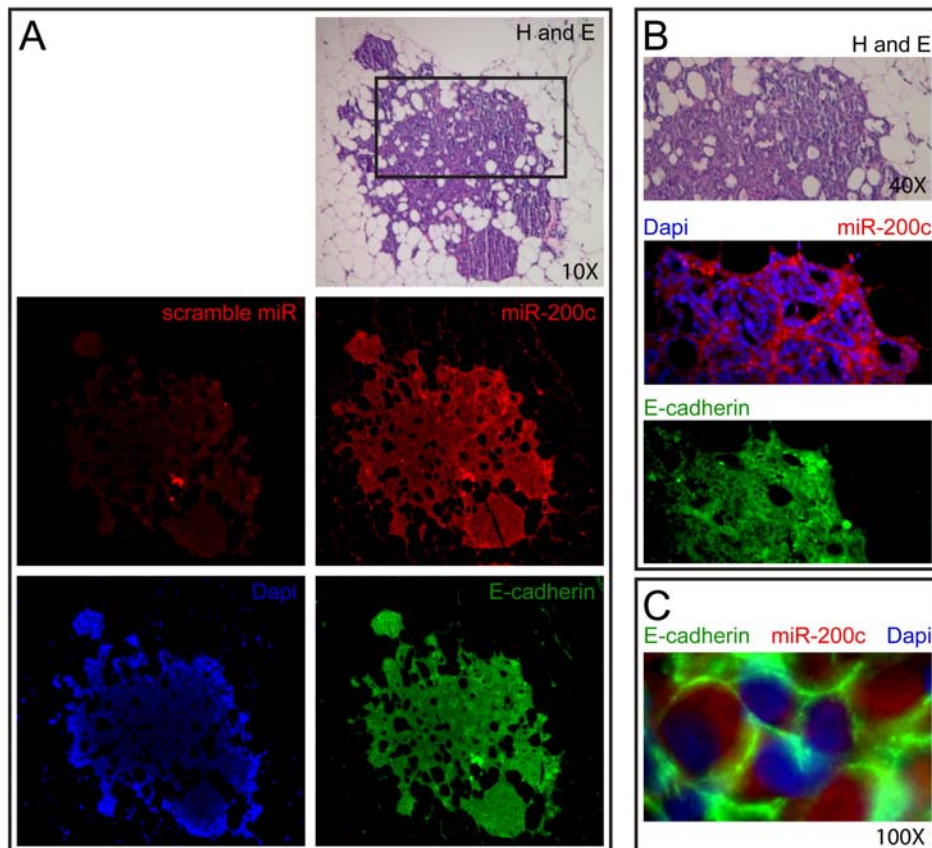


Fig. S16. MMTV-cErbB2-induced mammary adenocarcinomas express miR-200c and E-cadherin. **(A)** Microphotographs at 10X magnification, of Hematoxylin and Eosin (H and E) stained sections of a primary tumor (upper panel); in situ hybridization of a section from the same tumor, probed with scrambled miR (Left middle panel) or miR-200c (Right middle panel); DAPI (4',6-diamidino-2-phenylindole) and E-cadherin-stained tumor sections (Left and right lower panels respectively). Comparison of the in situ hybridization of scrambled miR and miR-200c revealed that miR-200c hybridizes specifically with MMTV-cErbB2-induced adenocarcinomas. **(B)** 40X magnification of the H and E stained (upper panel), miR-200c-hybridized and DAPI-stained (middle panel) and E-cadherin-stained section (lower panel) of an MMTV-cErbB2-induced mammary adenocarcinoma

(C) 100X magnification of overlapping images of a section of a primary MMTV-cErbB2-induced mammary adenocarcinoma, hybridized with miR-200c and stained with DAPI and E-cadherin. E-cadherin staining is localized at the plasma membrane, while miR-200c is localized in the cytoplasm.

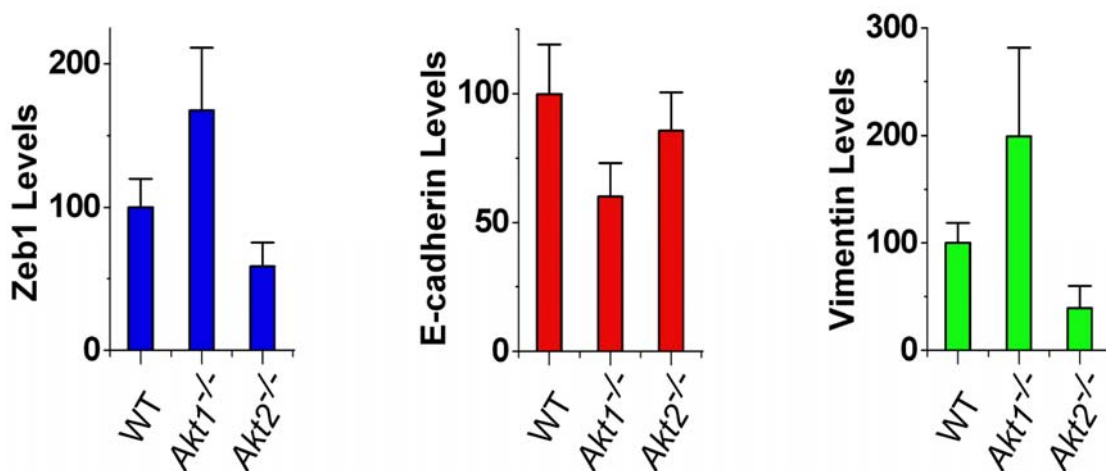


Fig. S17. MMTV-cErbB2/*Akt1*^{-/-} mammary adenocarcinomas have more Zeb1 and Vimentin and less E-cadherin than mammary adenocarcinomas developing in MMTV-cErbB2/*Akt1*^{+/+} and MMTV-cErbB2/*Akt2*^{-/-} mice. Western blots of primary tumor cell lysates were probed with the indicated antibodies and protein abundance was quantified using the Scion Image analysis software. The quantity of each protein is expressed as the ratio of the protein to tubulin. In tumors arising in wild type mice, the ratio was arbitrarily set to 1 (n=3 mice per group).

Supporting Tables

microRNA	AKT1	AKT2	AKT3	Function	Ref.
miR-27a	-1.76	-5.23	-2.43	Cell cycle	(1)
miR-149	-2.34	-3.56	-4.35	Oncogenic	(2)
miR-145	2.23	4.56	5.11	Insulin Receptor substrate (IRS1) target	(3)
miR-20a	0	-3.24	-2.54	Cell cycle	(4)
miR-17-5p	0	-3.12	-4.18	Cell cycle	(5)
miR-375	0	-2.25	-3.13	Phosphoinositide-Dependent Kinase 1 (PDK1) target	(6)
miR-15	-2.13	0	-4.23	B-Cell Lymphoma 2 (BCL2) target	(7)
miR-16	-2.45	0	-3.55	BCL2 target	(7)
miR-455	-3.65	0	-2.12	Adipocyte differentiation	(8)
miR-34a	-2.54	2.56	4.86	cell cycle-protein 53 (p53)	(9)
miR-34b	-2.88	2.87	4.31	cell cycle-p53	(9)
miR-34c	-2.53	2.52	3.87	cell cycle-p53	(9)
miR-200a	0	-3.05	0	EMT	(10, 11)
miR-200b	0	-3.46	0	EMT	(10, 11)
miR-200c	0	-5.43	0	EMT	(10, 11)
miR-141	0	-5.23	0	EMT	(10, 11)
miR-429	0	-3.32	0	EMT	(10, 11)
miR-449	0	-3.4	0	Endometrioid carcinoma	(12)
miR-433	0	2.12	0	Estrogen-Related Receptor gamma (ERRgamma) pathway	(13)
miR-532	0	2.34	0	Unknown	
miR-331	-2.45	0	0	Suppressor Of Cytokine Signaling 1 (SOCS1) target	(14)
miR-365	-2.13	0	0	Ultraviolet B (UVB) irradiation	(15)
miR-10b	-2.13	4.32	2.37	Metastasis	(16)

Table S1. The microRNA signatures of immortalized lung fibroblasts expressing a single Akt isoform at a time and responding to IGF1 differ. Cells were treated with IGF1 and they were harvested 16 hours later. The numbers indicate differences in abundance between unstimulated and IGF1-stimulated cells. MicroRNAs that changed in the same direction following IGF1 treatment of cells carrying any one of the three isoforms were clustered in groups, highlighted by different colors (column 1). Red indicates upregulation and blue downregulation (columns 2-4).

<u>miR</u>	<u>TKO</u>	<u>Akt1</u>
miR-20a	-3.21	0
miR-17-5p	-3.69	0
miR-375	-1.85	0
miR-34a	4.56	-2.54
miR-34b	4.11	-2.88
miR-34c	3.97	-2.54
miR-365	0	-2.13

<u>miR</u>	<u>TKO</u>	<u>Akt2</u>
miR-200a	0	-3.05
miR-200b	0	-3.46
miR-200c	0	-5.43
miR-141	0	-5.23
miR-429	0	-3.32
miR-449	0	-3.4
miR-433	0	2.12
miR-532	0	2.34
miR-15	-4.76	0
miR-16	-4.32	0
miR-455	-3.21	0

<u>miR</u>	<u>TKO</u>	<u>Akt1</u>	<u>Akt2</u>	<u>Akt3</u>
miR-27a	-1.88	-1.76	-5.23	-2.43
miR-149	-4.12	-2.34	-3.56	-4.35
miR-331	-3.26	-2.45	0	0
miR-145	0	2.23	4.56	5.11
miR-10b	0	-2.13	4.32	2.37

Table S2. Comparison of the microRNA signatures of triple Akt knockout (TKO) lung fibroblasts, and their derivatives expressing Akt1, Akt2 or Akt3. Cells were treated with IGF1 and harvested 16 hours later. The numbers indicate differences in abundance between unstimulated and IGF1-stimulated cells. The three panels show microRNAs which are upregulated (red) or downregulated (blue) differentially in response to IGF1, in TKO and Akt1-expressing cells (upper

panel), TKO and Akt2-expressing cells (middle panel) and TKO and Akt1, Akt2 and Akt3-expressing cells (lower panel) (see fig S2).

Supporting References

1. S. U. Mertens-Talcott, S. Chintharlapalli, X. Li, S. Safe, The oncogenic microRNA-27a targets genes that regulate specificity protein transcription factors and the G2-M checkpoint in MDA-MB-231 breast cancer cells. *Cancer Res* **22**, 11001-11011 (2007).
2. T. S. Wong, X. B. Liu, B. Y. Wong, R. W. Ng, A. P. Yuen, W. I. Wei, Mature miR-184 as Potential Oncogenic microRNA of Squamous Cell Carcinoma of Tongue. *Clin Cancer Res* **9**, 2588-2592 (2008).
3. B. Shi, L. Sepp-Lorenzino, M. Prisco, P. Linsley, T. deAngelis, R. Baserga, Micro RNA 145 targets the insulin receptor substrate-1 and inhibits the growth of colon cancer cells. *J Biol Chem* **45**, 32582-32590 (2007).
4. M. T. Pickering, B. M. Stadler, T. F. Kowalik, miR-17 and miR-20a temper an E2F1-induced G1 checkpoint to regulate cell cycle progression. *Oncogene* (2008).
5. N. Cloonan, M. K. Brown, A. L. Steptoe, S. Wani, W. L. Chan, A. R. Forrest, G. Kolle, B. Gabrielli, S. M. Grimmond, The miR-17-5p microRNA is a key regulator of the G1/S phase cell cycle transition. *Genome Biol* **8**, R127 (2008).
6. A. El Ouaamari, N. Baroukh, G. A. Martens, P. Lebrun, D. Pipeleers, E. van Obberghen, miR-375 targets 3'-phosphoinositide-dependent protein kinase-1 and regulates glucose-induced biological responses in pancreatic beta-cells. *Diabetes* **10**, 2708-2717 (2008).
7. A. Cimmino, G. A. Calin, M. Fabbri, M. V. Iorio, M. Ferracin, M. Shimizu, S. E. Wojcik, R. I. Aqeilan, S. Zupo, M. Dono, L. Rassenti, H. Alder, S. Volinia, C. G. Liu, T. J. Kipps, M. Negrini, C. M. Croce, miR-15 and miR-16 induce apoptosis by targeting BCL2. *Proc Natl Acad Sci U S A* **39**, 13944-13949 (2005).
8. T. B. Walden, J. A. Timmons, P. Keller, J. Nedergaard, B. Cannon, Distinct expression of muscle-specific microRNAs (myomirs) in brown adipocytes. *J Cell Physiol* **2**, 444-449 (2009).
9. L. He, X. He, L. P. Lim, E. de Stanchina, Z. Xuan, Y. Liang, W. Xue, L. Zender, J. Magnus, D. Ridzon, A. L. Jackson, P. S. Linsley, C. Chen, S. W. Lowe, M. A. Cleary, G. J. Hannon, A microRNA component of the p53 tumour suppressor network. *Nature* **7148**, 1130-1134 (2007).
10. P. A. Gregory, A. G. Bert, E. L. Paterson, S. C. Barry, A. Tsykin, G. Farshid, M. A. Vadas, Y. Khew-Goodall, G. J. Goodall, The miR-200 family and miR-205 regulate epithelial to mesenchymal transition by targeting ZEB1 and SIP1. *Nat Cell Biol* **5**, 593-601 (2008).
11. S. M. Park, A. B. Gaur, E. Lengyel, M. E. Peter, The miR-200 family determines the epithelial phenotype of cancer cells by targeting the E-cadherin repressors ZEB1 and ZEB2. *Genes Dev* **7**, 894-907 (2008).
12. W. Wu, Z. Lin, Z. Zhuang, X. Liang, Expression profile of mammalian microRNAs in endometrioid adenocarcinoma. *Eur J Cancer Prev* **1**, 50-55 (2009).

13. G. Song, L. Wang, Transcriptional mechanism for the paired miR-433 and miR-127 genes by nuclear receptors SHP and ERRgamma. *Nucleic Acids Res* **18**, 5727-5735 (2008).
14. D. L. Zanette, F. Rivadavia, G. A. Molfetta, F. G. Barbuzano, R. Proto-Siqueira, W. A. Silva-Jr, R. P. Falcao, M. A. Zago, miRNA expression profiles in chronic lymphocytic and acute lymphocytic leukemia. *Braz J Med Biol Res* **11**, 1435-1440 (2007).
15. L. Guo, Z. X. Huang, X. W. Chen, Q. K. Deng, W. Yan, M. J. Zhou, C. S. Ou, Z. H. Ding, Differential Expression Profiles of microRNAs in NIH3T3 Cells in Response to UVB Irradiation. *Photochem Photobiol* (2008).
16. L. Ma, J. Teruya-Feldstein, R. A. Weinberg, Tumour invasion and metastasis initiated by microRNA-10b in breast cancer. *Nature* **7163**, 682-688 (2007).